

Original Research Article

Accuracy-dependent dose-constraints and dose-based safety margins for organs-at-risk in radiotherapy

Joep C. Stroom^{a,*}, Sandra C. Vieira^a, Carlo Greco^a, Sebastiaan M.J.J.G. Nijsten^b^a Department of Radiation Oncology Champalimaud Centre for the Unknown Lisbon Portugal^b Radiotherapy Department MAASTRO Clinic Maastricht the Netherlands

ARTICLE INFO

Keywords:

OAR dose constraints
Treatment uncertainties
OAR safety margins
Error simulations
Recipes

ABSTRACT

Background and purpose: Geometrical uncertainties in radiotherapy are generally accounted for by margins for tumors, but their effect on organs-at-risk (OARs) is often ignored. We developed a model that incorporates dose- and geometry-based uncertainties in OAR planning using dose constraints.

Materials and methods: Radiotherapy uncertainties cause real dose-volume histograms (DVHs) to spread around the planned DVH. With a *published* OAR dose constraint $D(V_{crit}) < D_{crit}$ such that complication probability $< Y\%$, real differences from planned D_{crit} can be described by mean- (MD_{Dcrit}) and standard deviations (SD_{Dcrit}). Assuming complications are associated with the worst DVHs, *New* dose constraints that maintain complication probability can be derived for new treatments:

$$D_{crit,New} = D_{crit,publ} + \Phi^{-1}(1 - Y\%) * (SD_{Dcrit,publ} - SD_{Dcrit,New}) + (MD_{Dcrit,publ} - MD_{Dcrit,New}),$$

with $\Phi^{-1}(x)$ the inverse cumulative normal distribution function. Setting $SD_{Dcrit,New} = MD_{Dcrit,New} = 0$ in the recipe yields the “True” critical dose, and $D_{crit,True} - D_{crit,publ}$ can be considered a dose-based safety margin (DSM).

As hypothetical example, we estimated MD_{Dcrit} and SD_{Dcrit} values by simulating geometric errors in our clinical treatment plans and adding dose-based uncertainty. Over 1000 OARs with 108 different regular- and hypofractionation constraints were simulated. We assumed accuracy SDs to change from 2.5mm/3% to 1.5mm/2%.

Results: Results varied per OAR, fractionation, and constraint-type. If our 2.5mm/3% MD_{Dcrit} and SD_{Dcrit} values approximated dose-constraint studies, on average the DSM would be 4.5 Gy (18%) and our dose constraints would increase with 1.2 Gy (5%).

Conclusions: We introduced a first model relating dose constraints and complication probabilities with treatment uncertainties and safety margins for OARs. Among other things, it quantified how higher constraints can be applied with increasing radiotherapy accuracy.

1. Introduction

Radiotherapy uncertainties are traditionally accounted for by safety margins around the clinical target volume (CTV) yielding a planning target volume (PTV) [1–4], but are still subject of investigation [5]. For Organs-at-Risk (OAR) similar margins were introduced with the planning-organ-at-risk (PRV) concept [1] but they are often ignored in practice, also because their validity is less obvious [6]. Both PTV and PRV are only indirectly supplying safety; the *geometric* margins are supposed to give us a certain probability of *dose-delivery* accuracy in CTV

or OAR, and subsequently a high tumor control or low toxicity. The quantification of these margins using recipes has mainly been established using simulations and are to some extent arbitrary, e.g. margin recipes that allow a 5% underdosage in 10% of patients [3] have, to our knowledge, never been clinically shown to guarantee e.g. a $(1 - 10\%) = 90\%$ tumor control probability (TCP), not even using small animal models [7].

For many OARs, dose-effect studies have been performed plotting dose vs normal tissue complication probability (NTCP), which is often used to select a proper dose threshold with acceptable NCTP. These

* Corresponding authors at: Department of Radiation Oncology, Champalimaud Centre for the Unknown, Av. De Brasília s/n (Doca de Pedrouços), 1400 - 038 Lisboa, Portugal.

E-mail address: joep.stroom@fundacaochampalimaud.pt (J.C. Stroom).

<https://doi.org/10.1016/j.phro.2025.100713>

Received 5 June 2024; Received in revised form 2 November 2024; Accepted 23 January 2025

Available online 27 January 2025

2405-6316/© 2025 Published by Elsevier B.V. on behalf of European Society of Radiotherapy & Oncology. This is an open access article under the CC BY-NC-ND license (<http://creativecommons.org/licenses/by-nc-nd/4.0/>).

constraints are at the core of radiation treatment plans, and generally imply that the dose in a critical volume of an OAR must be smaller than a certain critical dose. Well known published dose constraints are collected by Quantec for regular fractionation treatments [8] and Timmerman [9] or Hytec [10] for hypo-fractionated radiotherapy. To increase their applicability, methods have been developed to convert existing constraints to different fractionation schemes and treatment modalities [11]. Since these dose–effect studies require considerable effort and patient numbers, they are relatively rare, and often constraints are used that were determined from data acquired years or even decades ago, when treatment techniques and accuracy were significantly different from now. Intuitively, current treatment accuracy should be higher and might allow for higher doses. However, to our knowledge, no publications have tried to quantify the dependency of dose constraints on treatment accuracy.

In this study, we aim to investigate how dose constraints relate to treatment uncertainties and develop a dose-based margin recipe for OARs in the process. The recipe should demonstrate how dose constraints can be adjusted for changes in radiotherapy accuracy. We then aim to show its usefulness by applying the model to our own clinical data.

2. Materials and methods

2.1. Derivation of constraint correction and OAR margin recipes

Our main assumption is that complications in dose–effect studies originated from those patients with the highest OAR doses. A second assumption is that the final error distributions involved can be approximated by Gaussians.

Imagine a planned DVH exactly fulfilling an OAR dose constraint denoted as $DX < D_{crit}$ Gy, guaranteeing an NTCP < Y%. DX can be D_{max} ,

D_{mean} , or D_{Vcrit} . In reality, geometry- and dose-based treatment uncertainties will give a distribution of possible, actually delivered DVHs around this planned DVH (Fig. 1A). This also yields a distribution of possible DX -values, which we characterize by standard deviation SD_{DX} around a mean deviation MD_{DX} . MD_{DX} can be positive or negative.

Ignoring inter-patient variations in planning and anatomy (Supplementary Material 1 (SM1)), let the DVHs belong to the published dose–effect study that set the dose constraint. Then if we consider the worst Y% of DVHs to be responsible for the Y% complications, we can determine the True constraint, i.e., the actual, fixed threshold above which complications occur. This True constraint has a dose value $\Phi^{-1}(1 - Y\%) \times SD_{DX,publ} + MD_{DX,publ}$ higher than the planned constraint (Fig. 1B), with $\Phi^{-1}(1 - Y\%)$ the inverse cumulative normal distribution function that gives the threshold (in SD) corresponding to the Y% largest values in a normal distribution. Hence:

$$D_{crit, True} = D_{crit, publ} + \Phi^{-1}(1 - NTCP) \times SD_{Dcrit, publ} + MD_{Dcrit, publ} \quad (1)$$

This recipe shows that since normally $NTCP < 15\%$ (so $\Phi^{-1}(1 - NTCP) > 1$) and $-MD_{Dcrit, publ} < SD_{Dcrit, publ}$, the True constraint is generally higher than the published constraint. Since $\Phi^{-1}(1 - 50\%) = 0$, $D_{crit, True} = TD50$ (dose with 50% probability of complications [8]) if $MD_{Dcrit, publ} = 0$. Furthermore, the difference between True- and planning-constraint can be considered a (dose-based) safety margin (DSM) for treatment uncertainties for OARs, i.e.

$$DSM_{publ} = D_{crit, True} - D_{crit, publ} = \Phi^{-1}(1 - NTCP) \times SD_{Dcrit, publ} + MD_{Dcrit, publ} \quad (2)$$

not unlike PTV margins for CTVs; it guarantees that despite treatment uncertainties, complications are limited to NTCP%, just as PTV margins might promise e.g. a TCP decrease of maximally 1% [4].

If treatment uncertainties change but we maintain NTCP, a New

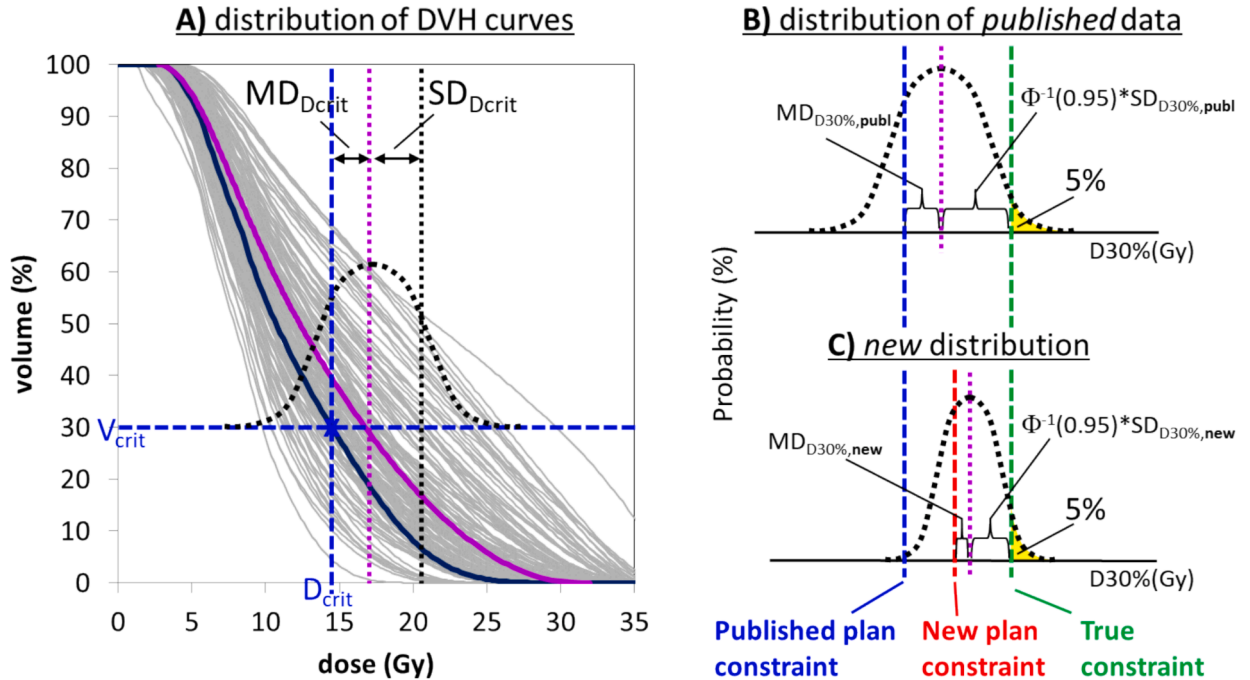


Fig. 1. Illustration of how Eqs. (1), (2), and (3) were derived. In A) a planned OAR DVH (black curve) exactly fulfilling a hypothetical dose constraint of $D30\% \leq 14.7$ Gy (blue cross). A distribution of DVH curves due to dose- and geometry-based uncertainties are shown by grey curves, with the mean curve in purple. A bell-curve indicates the distribution of $D30\%$, with MD_{Dcrit} and SD_{Dcrit} the mean and standard deviations from the plan. In B) a larger normal distribution of $D30\%$ for published dose–effect data in the past is shown. Assuming an accepted 5% NTCP for this OAR, and that the 5% worst DVHs (yellow area) cause the complications, the True dose constraint (dashed green line) is larger than the published constraint by a dose-based safety margin $DSM_{publ} = MD_{D30\%,publ} + \Phi^{-1}(1 - 5\%) \times SD_{D30\%,publ}$, with Φ^{-1} the inverse cumulative normal distribution function (Eq. (1)). In C) a new distribution with smaller uncertainties is indicated; maintaining a 5% NTCP yields a New plan constraint equal to the True constraint minus the smaller $DSM_{New} = MD_{D30\%,New} + \Phi^{-1}(1 - 5\%) \times SD_{D30\%,New}$ (dashed red line, Eq. (3)). (For interpretation of the references to color in this figure legend, the reader is referred to the web version of this article.)

constraint can be derived that is $DSM_{New} = \Phi^{-1}(1 - Y\%) \times SD_{DX,New} + MD_{DX,New}$ Gy smaller than $D_{crit,True}$, yielding a constraint correction recipe (Fig. 1C):

$$D_{crit,New} = D_{crit,publ} + \Phi^{-1}(1-NTCP) \times (SD_{Dcrit,publ} - SD_{Dcrit,New}) + (MD_{Dcrit,publ} - MD_{Dcrit,New}). \quad (3)$$

This equation effectively subtracts DSM_{New} from DSM_{publ} , hence eliminating $D_{crit,True}$. It demonstrates that if actual treatment accuracy is higher than during assessment of the published constraint, we can generally relax (i.e. increase) the constraints while maintaining NTCP (and vice versa). Maintaining the constraint will give a better (lower) NTCP than already accepted.

2.2. Obtaining treatment accuracy data

The three variables in Eqs. (1), (2) and (3) are the accepted NTCP, which should be reported together with the published dose constraints [8], and the variations in the critical doses (MD_{Dcrit} , SD_{Dcrit}). To illustrate our model, we estimated MD_{Dcrit} and SD_{Dcrit} using our own clinical treatment plans. We simulated geometrical errors SD_{geo} , containing systematic (Σ) and random (σ) components [12–14] that apply dose shifts and convolutions [15], respectively, and determined the resulting critical dose variations ($SD_{Dcrit,Geo}$) for all relevant OARs. For comparisons, we also calculated relative values: $SD_{Dcrit,geo}(\%) = SD_{Dcrit,geo}(Gy) / D_{crit}(Gy)$ and $MD_{Dcrit}(\%) = MD_{Dcrit}(Gy) / D_{crit}(Gy)$. Dose errors $SD_{Dcrit,dos}(\%)$ [16–19] were added quadratically to $SD_{Dcrit,geo}(\%)$ to get the total $SD_{Dcrit,Tot}(\%)$:

$$SD_{Dcrit,Tot} = \sqrt{SD_{Dcrit,Dos}^2 + SD_{Dcrit,Geo}^2}. \quad (4)$$

To correlate geometric error with OAR dose error, we linearly fitted MD_{Dcrit} and SD_{Dcrit} as function of $SD_{geo}(mm)$, yielding slopes S_{MD} and S_{SD} (in %/mm) and offsets O_{MD} and O_{SD} (in %), e.g. $SD_{Dcrit}(\%) = O_{SD}(\%) + S_{SD}(\%/mm) \times SD_{geo}(mm)$ (see Fig. 2C,G,K). Further details are described in SM2.

2.3. Application of the recipes

1) The slopes and offsets from abovementioned *linear fits* were averaged overall and per constraint group (by fractionation and type), and were subsequently entered into Eq. (1) using Eq. (4), yielding a direct relation between treatment uncertainties $SD_{geo}(mm)$ and $SD_{dos}(\%)$, and the relative OAR safety margin:

$$\frac{D_{crit,True}}{D_{crit,publ}} = 1 + \Phi^{-1}(1 - NTCP) \times \sqrt{SD_{Dcrit,Dos}^2 + (O_{SD} + S_{SD} \times SD_{Geo})^2} + O_{MD} + S_{MD} \times SD_{Geo} \quad (5)$$

A similar relation can be determined for $D_{crit,New} / D_{crit,publ}$. We then applied these equations with NTCP = 1%, NTCP = 10%, and with average NTCP per constraint group, for geometry- and dose-based uncertainties (1SD) varying from 0.5mm/1% to 4.5mm/5%, respectively.

2) Our estimates of $SD_{Dcrit,Tot}$ and $MD_{Dcrit,Tot}$ ($= MD_{Dcrit,Geo}$) for each simulated OAR separately were also used to *directly calculate* True dose constraints, dose safety margins, and New dose constraints for our OARs using Eqs. (1), (2) and (3). We assumed that due to technology advances uncertainties decreased by 1 mm and 1%, from 2.5mm/3% to 1.5mm/2%, and averages per constraint were calculated. Since it is practically impossible to obtain MD_{Dcrit} and SD_{Dcrit} for published dose-effect studies, we assumed the results from our 2.5mm/3% calculations were representative of these values.

2.4. Treatment plan data

To include inter-patient variations per OAR (see also SM1), we

simulated the systematic and random errors on 552 plans of 348 patients yielding data for 1005 OARs. The plans were generated with Eclipse v15 (Varian Medical Systems), generally with 4 Volumetric Arc Therapy (VMAT) arcs, PTV margins of 3 to 5 mm, and using the AAA calculation model. For 396 hypo-fractionated-plans there were on average 1.9 relevant (i.e. critical) OARs per plan, in 156 regular-plans we found 1.6 relevant OARs per plan. See SM2 and SM3 for more details. Our clinically used physical dose constraints ($D_{crit,publ}$) were taken from Quantec [8] for regular fractionations and Timmerman [9] for hypo-fractionated treatments. NTCP was taken from the publications when available [7,20], and assumed to be 5% when not.

3. Results

3.1. True and New constraints from linear fits

Correlation between geometric variations and its effect on OAR dose was fairly linear in our treatment plans. Mean residual fitting error was <1% (relative to the critical dose) in all constraint groups and average correlation coefficients (R^2) for slopes >0.1 Gy/mm vary from 83% for MD_{Dmax} to 95% for SD_{Dcrit} . In general, the slope S_{SD} depended on the steepness of the dose gradients around the OAR, whereas S_{MD} depended on the degree of critical dose conformity, as indicated by three examples in Fig. 2.

For Eq. (5), averaged over all our techniques, OARs, and constraints, the relative slope for *standard deviations* S_{SD} was 3.2 %/mm and average offset O_{SD} was 1.7%. For *mean deviations* values were $S_{MD} = 0.7 \%$ /mm and $O_{MD} = 0.5\%$. Table 1 shows average slopes and offsets per fractionation- and constraint-type. Single dose treatments displayed the highest sensitivity for motion reflecting the conformity of dose around the organ and the absence of dose convolutions for random errors, which tend to have a smoothing effect. Inversely, slopes for OARs in regularly fractionated plans were on average the lowest. The dose smoothing together with low dose conformity around the OAR could yield negative slopes especially for MD_{Dmax} (e.g. Fig. 2G).

Fig. 3 shows relative True and New constraints as function of treatment error using slopes and offsets from Table 1 and Eq. (5). For NTCP = 1% ($\Phi^{-1} = 2.33$), overall mean $D_{crit,True}$ was 20% to 30% higher than $D_{crit,publ}$ in the 2mm/2.5% to 3mm/3.5% range of errors (Fig. 3A). For NTCP = 10% ($\Phi^{-1} = 1.28$) this increase was about 15% (C). New constraints show a similar drop in steepness of the overall curve. For the curves per group, single dose curves showed the largest changes, with a 17% drop in $D_{crit,New}$ for each 1mm/1% added uncertainty at NTCP = 1% (Fig. 3B), and a 10% drop at NTCP = 10% (Fig. 3D). In Fig. 3E,F, the curves with NTCPs per constraint group generally lie between NTCP = 1% and NTCP = 10% curves.

3.2. Effect of accuracy improvement using direct calculations

Table 2 shows a summary of the dose variation and constraint data for the 1005 OARs. Average D_{max} , D_{mean} , and DV constraints for regular- and hypo-Fx are indicated, corrected for the estimated 1mm/1% improvements in accuracy. For more detail, see SM4 with data per OAR. Results in Table 2 corresponded well with the linear fits from Fig. 3E,F. DSMs in Table 2 were on average 18% (4.5 Gy), varying from 7% (3.2 Gy) for regular DV-constraints to 44% (7.0 Gy) for single dose D_{max} . As expected, small OARs with the smallest NTCP showed the largest values (SM4). A 1mm/1% accuracy increment would increase our constraints on average with 5% (1.2 Gy), varying from 2% (1.0 Gy) for regular DV-constraints to 12% (1.9 Gy) for single dose D_{max} . For all OARs and techniques the estimated constraints increased (SM4).

4. Discussion

This paper is a first attempt to link published dose constraints to treatment uncertainties and margins for OARs. Using the uncertainties

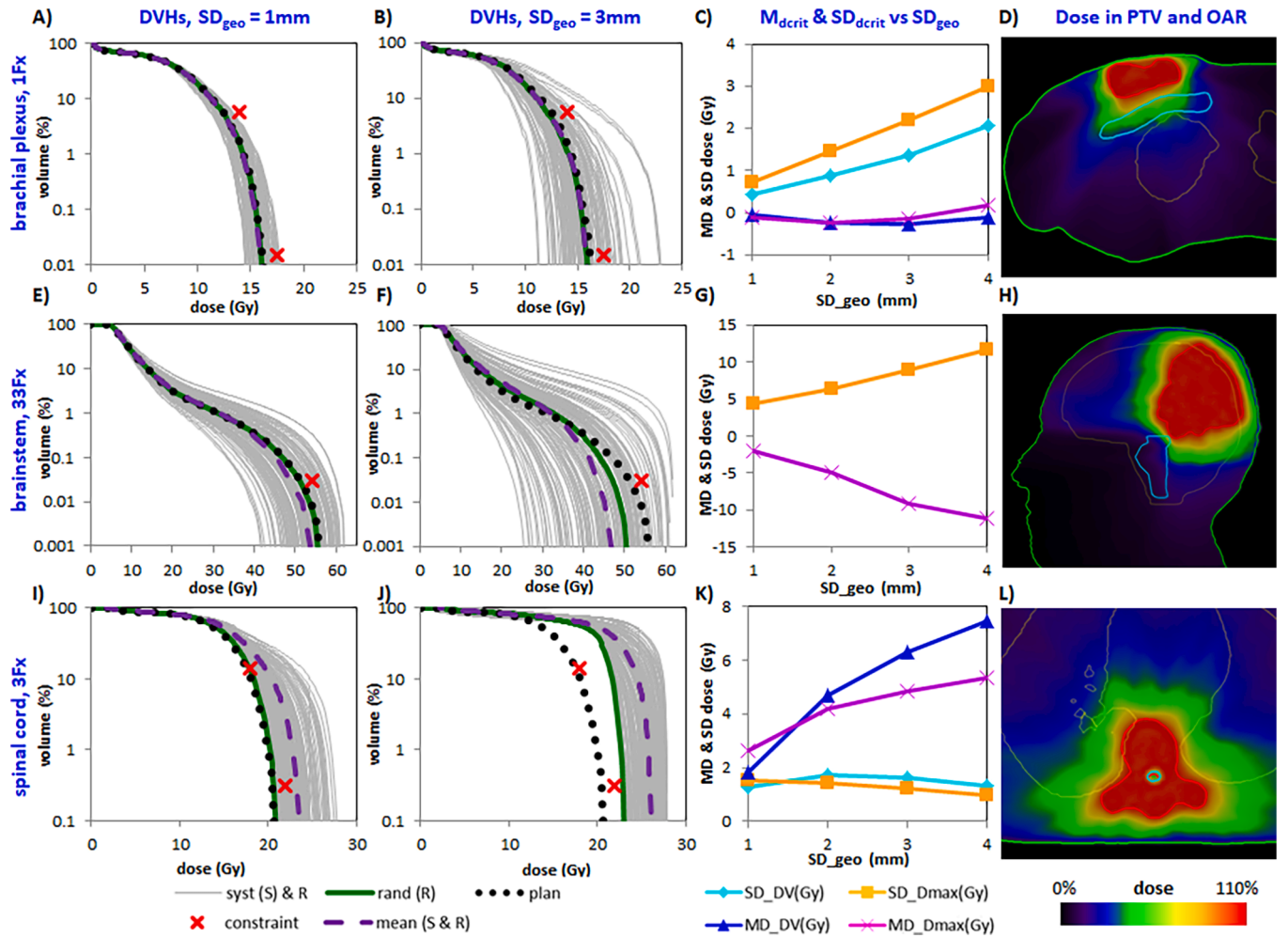


Fig. 2. Three examples (A-D, E-H, I-L) of the effect of motion simulation on dose in OARs. For all cases the DVHs for 1 mm and 3 mm SD_{geo} are shown in the first two images per row. Dotted are the planned DVHs, green the effect of random deviations (R) only, grey the effect of systematic deviations (S) in the random-error-corrected dose, purple the average of the grey curves, and the red crosses are the published dose constraints. To better illustrate near D_{max} (in 0.008 cm^3), the volume axis is logarithmic. The third image shows the relation between SD_{geo} and MD_{dcrit} or SD_{dcrit} from which linear fits are derived. The fourth image depicts a slice of the planned dose through the relevant OAR (in light blue). The 1-Fx brachial plexus case shows a moderate increase in SD_{dcrit} with increasing SD_{geo} , and no change in MD_{dcrit} . The 33-Fx brainstem case is an extreme example of decreasing MD_{dcrit} due to the non-conformity of the high dose, whereas the 3-Fx spinal cord case is an extremely conform high-dose distribution example. (For interpretation of the references to color in this figure legend, the reader is referred to the web version of this article.)

in critical doses (SD_{dcrit} and MD_{dcrit}) and the accepted NTCP, a recipe has been developed to calculate a “True” constraint (Eq. (1)), from which a dose-based safety margin (DSM) can be derived (Eq. (2)). The recipes indicate that if published dose-constraints are not adjusted for treatments plans with uncertainties that differ from those during dose-constraint determination, then actual NTCPs will deviate from the published one. Eq. (3) enables us to do this adjustment, which can help to avoid having to repeat cumbersome dose–effect studies each time we change our treatments.

True constraints would be useful in probabilistic treatment planning that takes uncertainties into account during optimization [21–23]. Applying the recipes to our own, generally decades-old, dose constraints with simulated uncertainty estimates suggested that our average DSM was about 4.5 Gy and that assuming a modest 1mm/1% reduction in geometry/dose variations, our constraints could be on average 1.2 Gy higher than the published values while maintaining NTCP (Table 2). This confirms our clinical experience where complication probabilities seem to be lower than predicted [24]. Also, published, updated constraints tend to be relaxed compared to the original values [25–28].

Two main assumptions were made in our model. Firstly, the worst NTCP% DVH curves are assumed to represent the accepted NTCP% of

cases with toxicity. In reality, individual radio-sensitivity will also determine the OAR response, but this should average out for large datasets and moderately-sized sensitivity variation; for tumors, van Herk et al found no significant effect of radio-sensitivity variations on safety margins for geometric uncertainties [4]. For OARs, it is conceivable that large radio-sensitivity variations will increase total variations and hence D_{True} ¹ and reduce the effect of treatment accuracy improvements ($D_{New} - D_{pub}$). However for now, the influence of radio-sensitivity variation is beyond the scope of the present paper, and is subject of further study [29]. Secondly, the distribution of SD_{dcrit} is assumed Gaussian, which makes further calculation easier, resulting in

¹ Actually, there is one OAR in Quantec [8] with a TD50-value that we can compare to our estimated D_{True} (see Eq. (1)): for spinal cord D_{max} from Quantec, TD50 = 69 Gy. Since these are values for regular fractionation (2 Gy/Fx), LQ-conversion of 69 Gy from 34.5 to 25 fractions with $\alpha/\beta = 2 \text{ Gy}$ would yield 62 Gy. This is actually equal to our prediction (SM4), which would indicate that for this OAR and these treatments radio-sensitivity variation is less relevant than geometric/dosimetric variations and/or that the simulated 2.5mm/3% uncertainty was too high.

Table 1

Slopes and offsets of linear fits to convert geometric variation (mm) to mean- (MD) and standard (SD) deviations in critical dose (%) for various prescription types and for Dose-Volume (DV)-, D_{\max} -, and D_{mean} -critical doses, averaged over the OARs. Standard deviations are in small, grey.

prescription	DV					D_{\max}					D_{mean}				
	n	offset (%)		slope (%/mm)		n	offset (%)		slope (%/mm)		n	offset (%)		slope (%/mm)	
		O_{SD}	O_{MD}	S_{SD}	S_{MD}		O_{SD}	O_{MD}	S_{SD}	S_{MD}		O_{SD}	O_{MD}	S_{SD}	S_{MD}
regular	95	0.5 ^{2.0}	0.5 ^{1.8}	1.9 ^{1.7}	-0.5 ^{1.5}	86	0.9 ^{2.1}	0.8 ^{1.8}	1.5 ^{1.3}	-1.1 ^{1.9}	70	0.5 ^{1.1}	0.2 ^{1.4}	4.1 ^{1.9}	0.0 ^{1.0}
hypo 1F	164	-0.1 ^{2.6}	-1.9 ^{3.4}	5.2 ^{4.1}	3.1 ^{5.0}	289	5.4 ^{5.1}	1.4 ^{4.1}	5.0 ^{2.8}	3.3 ^{4.1}					
hypo 3F	87	0.9 ^{2.5}	-0.9 ^{2.4}	3.8 ^{1.9}	1.9 ^{3.6}	190	3.4 ^{4.5}	2.6 ^{2.9}	2.3 ^{1.7}	-0.4 ^{3.4}					
hypo 5F	133	1.5 ^{2.8}	-0.3 ^{2.5}	3.2 ^{1.9}	1.4 ^{3.1}	197	1.9 ^{2.8}	2.0 ^{2.3}	1.8 ^{1.4}	-1.4 ^{2.1}					
average	120	0.7 ^{2.5}	-0.6 ^{2.5}	3.5 ^{2.4}	1.5 ^{3.3}	191	2.9 ^{3.6}	1.7 ^{2.8}	2.6 ^{1.8}	0.1 ^{2.9}	70	0.5 ^{1.1}	0.2 ^{1.4}	4.1 ^{1.9}	0.0 ^{1.0}

Eqs. (1), (2), and (3). However, the distribution of SD_{Dcrit} can be somewhat skewed depending on position and shape of the OAR with respect to the dose distribution.

We applied simulations to convert geometric errors SD_{Geo} to deviations in D_{crit} and then added dose errors SD_{Dos} . Considering that in practice $SD_{\text{Dos}}(\%)$ is about equal to $SD_{\text{Geo}}(\text{mm})$, Eq. (5) and Table 1 imply that for our OARs geometric errors were on average about 3 times more important than the dose errors. Furthermore, on average our relevant OARs receive more dose than planned ($MD > 0$), implying that some degree of conformal avoidance (Fig. 2I-L) was more likely than not (Fig. 2E-H). Largest D_{crit} deviations were found in the single dose group although comparing regular with hypo fractionation is complicated because not only patient groups but also constraints were truly different.

Obtaining geometric deviations $MD_{\text{Dcrit,Geo}}$ and $SD_{\text{Dcrit,Geo}}$ for the published dose-effect data from decades ago is practically impossible. Using our own treatment plans, we actually calculated dose constraint changes corresponding to changes in our particular treatment accuracy, which can only be a first approximation of dose-effect studies. It is likely that our treatment plans are more conformal to OARs with steeper dose gradients than in the past (e.g. Fig. 2L), resulting in too high DSMs by increased slopes S_{SD} and S_{MD} (Eq. (5)). Therefore we assumed a modest 2.5mm/3% uncertainty at constraint publication and only a 1mm/1% accuracy improvement¹. We also underestimated $SD_{\text{Dcrit,Geo}}$ somewhat by not fully including inter-patient variability (SM1). Should another accuracy appear more appropriate, Fig. 3E,F quickly estimates the consequences, e.g., overall DSM would change from 18% to 22% if initial accuracy would be 3.5mm/4% instead of 2.5mm/3%.

Regarding geometric simulations with OARs, we assumed $\Sigma = \sigma$, dose invariance with shifts, and approximated 3F and 5F random errors by convolutions, which are approximations as well (SM2). Furthermore, we assumed equal uncertainties for all OARs, which might e.g. explain the high dose-based margins for spinal cord and small organs in the brain. Finally, for 10 of 69 constraints we only had 1 or 2 cases (SM4), questioning how well our patient cohort was represented. Therefore, the validity of our simulations and subsequent results should only be seen as a first indication of what could be happening and needs

to be refined and independently confirmed using RT plans from different periods and institutions. Readers should interpret the results presented with caution.

Eq. (2) is similar to published PTV margin recipes for geometrical uncertainties of the CTV, a difference being that PTV-margins do not include dose uncertainties. But more importantly, since in the end tumor and OAR doses are what matters, chosen *geometric* thresholds need a *dose-based* justification, based on, e.g., adequate average dose coverage of the CTV [2], a CTV underdosage in e.g. 10% of the patient population [3], or an estimated TCP decrease of e.g. 1% [4]. However, these are indirect justifications with rather arbitrary thresholds and/or models still without clinical foundation. In other words, PTV margin recipes do not contain a TCP-variable linking margins to clinical outcome. In contrast, the OAR margin recipe presented in Eq. (2) is based directly on clinical dose-effect data with known NTCPs.

One consequence of Eq. (2) is that steeper dose gradients contribute less to organs at risk sparing than we might expect. Steeper dose gradients yield a higher $SD_{\text{Dcrit,Geo}}$, and larger margins are then acquired to achieve the same OAR dose sparing. Actually, the same reasoning applies to the use of steep gradients around CTV-to-PTV margins [30]. A further consequence is that PRV margins become less relevant [6]: it is superfluous to apply extra geometric margins for OAR position uncertainty that is already included in the dose constraints (but in plan optimization, PRVs can still usefully guide dose away from OARs). Only in cases and institutions where the new accuracy is less than during dose-effect studies ($SD_{\text{Dcrit,New}} > SD_{\text{Dcrit,publ}}$ in Eq. (3)) or where for medical reasons *more caution* is desirable in a particular patient, larger margins might be required. In the latter case, or when *less caution* is accepted (e.g. in re-irradiation), one can simply adjust the NTCP in Eq. (3).

Eq. (3) can also apply to treatment plan QA. Measured 3D dose distributions can generate measured DVHs that should be evaluated using dose-constraints $D_{\text{crit,Meas}}$. Measurement uncertainties $MD_{\text{Dcrit,meas}}$ and $SD_{\text{Dcrit,Meas}}$ should be determined per measurement technique. For instance, portal dosimetry systems exist that calculate 3D dose distributions and DVHs from measured 2D portal images, using pre-treatment

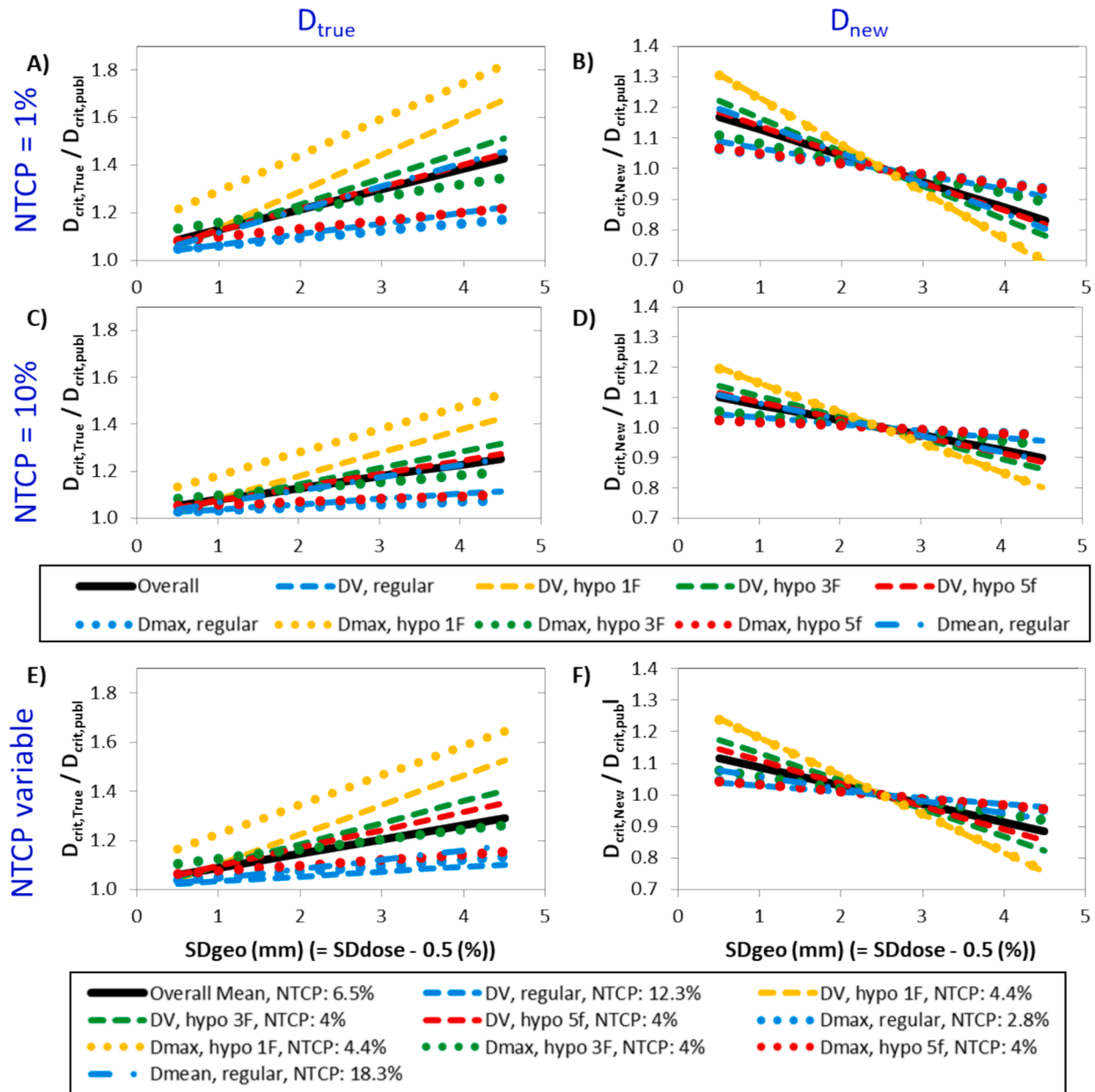


Fig. 3. Ratios $D_{crit, True} / D_{crit, publ}$ (Eq. (5), Figs. A,C,E) and $D_{crit, New} / D_{crit, publ}$ (Figs. B,D,F) as function of treatment uncertainty for various values of NTCP: 1% in Figs A,B, 10% in Figs C,D, and variable with constraint group (Table 2) in Figs. E,F. We assumed 2.5mm/3% uncertainties during constraint publications for calculation of $D_{crit, New} / D_{crit, publ}$. For simplicity's sake we assumed that geometric uncertainty in mm changed as dose-based uncertainty minus 0.5 in %. Dashed and dotted curves represent averages for the different constraint groups: regular with Quantec constraints, and hypo-fractionation with Timmerman constraints, each with a different color. The overall mean curve is also shown (solid black), the curves for the individual constraint groups are calculated similarly using the slopes and offsets from Table 1.

Table 2

Summary of published, True, and New constraints after applying the recipes (Eqs. (1) and (3)) to Timmerman (hypoFx) and Quantec (regularFx) constraints assuming geometry/dose uncertainties decreased from 2.5mm/3% during publication to 1.5mm/2% currently. Columns indicate the constraint types, #OARs summarized, # calculations per OAR, standard- (SD) and mean-deviation (MD) of critical dose Dcrit @publication and currently, NTCP, published critical dose, and dose increase for True and New constraints in Gy and %. DSM is the dose-based safety margin obtained by subtracting published constraints from True constraints. Average values per constraint group are given, with the standard deviation in small, grey.

published, True, and New constraints		# OAR	# / OAR	SD _{Dcrit} (Gy)		MD _{Dcrit} (Gy)		NTCP (%)	Published constraint (Gy)	change (Gy) with published		change (%) with published	
				2.5mm /3%	1.5mm /2%	2.5mm /3%	1.5mm /2%			True (DSM)	New	True (DSM)	New
quantec	D _{max}	4	22	3.6 0.9	2.5 0.7	-0.5 1.1	-0.1 0.8	2.8 1.7	54.8 3.6	6.9 3.6	1.8 1.1	12.6 6.5	3.3 1.9
	D _{mean}	3	23	3.8 2.7	2.5 1.9	-0.1 0.2	0.1 0.1	18.3 10.3	25.7 15.5	2.5 1.1	0.7 0.4	9.7 4.5	2.6 1.4
	DV	7	14	2.8 0.6	1.8 0.5	-0.3 0.3	0.0 0.2	12.3 9.4	46.9 15.7	3.2 1.5	1.0 0.7	6.9 3.1	2.1 1.4
timmerman	1Fx D _{max}	14	17	3.1 0.6	2.3 0.4	1.6 1.3	1.1 0.9	4.4 1.3	16.1 3.3	7.0 2.1	1.9 0.6	43.6 12.9	11.6 3.6
	3Fx D _{max}	17	11	2.5 0.8	2.0 0.8	1.2 2.2	1.1 1.5	4.0 1.7	26.3 6.6	5.8 3.4	1.1 0.6	22.1 12.9	4.2 2.4
	5Fx D _{max}	17	13	2.6 0.7	1.9 0.5	-0.5 0.9	0.0 0.6	4.0 1.7	34.9 6.6	4.2 1.0	0.8 0.2	12.0 2.9	2.3 0.7
	1Fx DV	15	17	1.4 0.6	0.9 0.4	0.4 0.5	0.2 0.2	4.4 1.3	12.9 3.1	2.9 1.7	1.2 0.8	22.9 13.6	9.5 6.2
	3Fx DV	15	11	1.8 0.7	1.2 0.5	0.8 1.2	0.5 0.6	4.0 1.7	20.5 6.1	4.2 2.3	1.5 0.9	20.5 11.2	7.1 4.6
	5Fx DV	16	13	2.1 0.7	1.4 0.5	0.4 0.8	0.3 0.5	4.0 1.7	26.0 7.7	4.2 1.9	1.3 0.6	16.1 7.4	5.1 2.3
average		12	16	2.6 0.9	1.8 0.7	0.3 0.9	0.4 0.6	6.5 3.4	29.3 7.6	4.5 2.1	1.2 0.7	18.5 8.3	5.3 2.7
SD		5	4	0.7 0.6	0.5 0.4	0.7 0.6	0.4 0.4	5.0 3.4	13.1 4.6	1.6 0.9	0.4 0.2	10.3 4.1	3.2 1.7

no-transmission images or in-vivo transmission images [31]. Each method will have its particular accuracy, and hence different dose-constraints and safety margins (Eq. (2)), either lower or higher than planning values.

A consequence of our methodology is that future dose–effect studies should not only be presenting their accepted toxicity probabilities (NTCP), which currently are not always present [9], but also an estimate of their (currently also lacking) treatment accuracy and preferably the variation in critical dose values (or TD50 and MD_{Dcrit}, see Eq. (1)). This allows calculating, and publishing, the True dose constraints (Eq. (1)) and the dose-based safety margins corresponding to the accepted NTCP (Eq. (2)), so that, ideally, individually-calculated critical dose variations can be used to generate corrected dose constraints more precisely and per institution; our results already vary significantly for different plans and OARs in one hospital. Hence, before clinical implementation, independent verification of the method either by different hospitals or using e.g. TD50 is strongly recommended.

In conclusion, our proposed method tries to demonstrate a novel way

to reappraise dose/volume constraints and OAR margins. The new methodology estimates True and New dose planning constraints from existing published constraints, and suggests a concept for OAR dose-based safety margins. It shows how, while maintaining the accepted NTCP, increased radiotherapy accuracy allows higher dose constraints (and vice versa).

CRediT authorship contribution statement

Joep C. Stroom: Conceptualization, Methodology, Software, Investigation, Writing – original draft, Funding acquisition. **Sandra C. Vieira:** Writing – review & editing, Methodology. **Carlo Greco:** Supervision, Writing – review & editing. **Sebastiaan M.J.J.G. Nijsten:** Writing – review & editing, Funding acquisition.

Declaration of competing interest

The authors declare that they have no known competing financial

interests or personal relationships that could have appeared to influence the work reported in this paper.

Acknowledgements

The work in this paper has been supported by a Varian Research Grant.

Appendix A. Supplementary data

Supplementary data to this article can be found online at <https://doi.org/10.1016/j.phro.2025.100713>.

References

- [1] Report ICRU. 50: prescribing, recording and reporting photon beam therapy. ICRU 1993. <https://www.icru.org/report/prescribing-recording-and-reporting-photon-beam-therapy-report-50/>.
- [2] Stroom JC, de Boer HC, Huizenga H, Visser AG. Inclusion of geometrical uncertainties in radiotherapy treatment planning by means of coverage probability. *Int J Radiat Oncol Biol Phys* 1999;43:905–19. [https://doi.org/10.1016/S0360-3016\(98\)00468-4](https://doi.org/10.1016/S0360-3016(98)00468-4).
- [3] van Herk M, Remeijer P, Rasch C, Lebesque JV. The probability of correct target dosage: dose-population histograms for deriving treatment margins in radiotherapy. *Int J Radiat Oncol Biol Phys* 2000;47:1121–35. [https://doi.org/10.1016/S0360-3016\(00\)00518-6](https://doi.org/10.1016/S0360-3016(00)00518-6).
- [4] van Herk M, Remeijer P, Lebesque JV. Inclusion of geometric uncertainties in treatment plan evaluation. *Int J Radiat Oncol Biol Phys* 2002;52:1407–22. [https://doi.org/10.1016/S0360-3016\(01\)02805-X](https://doi.org/10.1016/S0360-3016(01)02805-X).
- [5] Janssen TM, van der Heide UA, Remeijer P, Sonke J-J, van der Bijl E. A margin recipe for the management of intra-fraction target motion in radiotherapy. *Phys Imaging Radiat Oncol* 2022;24:159–66. <https://doi.org/10.1016/j.phro.2022.11.008>.
- [6] Stroom JC, Heijmen BJM. Limitations of the planning organ at risk volume (PRV) concept. *Int J Radiat Oncol Biol Phys* 2006;66:279–86. <https://doi.org/10.1016/j.ijrobp.2006.05.009>.
- [7] Kampfer S, Dobiasch S, Combs SE, Wilkens JJ. Development of a PTV margin for preclinical irradiation of orthotopic pancreatic tumors derived from a well-known recipe for humans. *Z Med Phys* 2023. <https://doi.org/10.1016/j.zemedi.2023.03.005>. S0939388923000429.
- [8] Marks LB, Yorke ED, Jackson A. Use of normal tissue complication probability models in the clinic. *Int J Radiat Oncol Biol Phys* 2010;76:S10–9. <https://doi.org/10.1016/j.ijrobp.2009.07.1754>.
- [9] Timmerman RD. An overview of hypofractionation and introduction to this issue of seminars in radiation oncology. *Semin Radiat Oncol* 2008;18:215–22. <https://doi.org/10.1016/j.semradonc.2008.04.001>.
- [10] Grimm J, Marks LB, Jackson A, Ten Haken RK, Constine LS, Eisbruch A, et al. High dose per fraction, hypofractionated treatment effects in the clinic (HyTEC): an overview. *Int J Radiat Oncol Biol Phys* 2021;110:1–10. <https://doi.org/10.1016/j.ijrobp.2020.10.039>.
- [11] Perkó Z, Bortfeld T, Hong T, Wolfgang J, Unkelbach J. Derivation of mean dose tolerances for new fractionation schemes and treatment modalities. *Phys Med Biol* 2018;63:035038. <https://doi.org/10.1088/1361-6560/aa9836>.
- [12] Greco C, Stroom J, Vieira S, Mateus D, Cardoso MJ, Soares A, et al. Reproducibility and accuracy of a target motion mitigation technique for dose-escalated prostate stereotactic body radiotherapy. *Radiother Oncol* 2021;160:240–9. <https://doi.org/10.1016/j.radonc.2021.05.004>.
- [13] Schick K, Sisson T, Frantzis J, Khoo E, Middleton M. An assessment of OAR delineation by the radiation therapist. *Radiography* 2011;17:183–7. <https://doi.org/10.1016/j.radi.2011.01.003>.
- [14] Amaoui B, Hadaoui A, Mouhssine D, Semghouli S. Evaluation of setup errors in conformal radiotherapy for pelvic tumours: Case of the Regional Center of Oncology, Agadir. *Radiat. Med. Prot.* 2020;1:99–102. <https://doi.org/10.1016/j.radmp.2020.05.003>.
- [15] Bel A, van Herk M, Lebesque JV. Target margins for random geometrical treatment uncertainties in conformal radiotherapy. *Med Phys* 1996;23:1537–45. <https://doi.org/10.1118/1.597745>.
- [16] Mijnheer B. Current clinical practice versus new developments in target volume and dose specification procedures: a contradiction? *Acta Oncol* 1997;36:785–8. <https://doi.org/10.3109/02841869709001357>.
- [17] Mijnheer BJ, Battermann JJ, Wambersie A. What degree of accuracy is required and can be achieved in photon and neutron therapy? *Radiother Oncol* 1987;8:237–52. [https://doi.org/10.1016/S0167-8140\(87\)80247-5](https://doi.org/10.1016/S0167-8140(87)80247-5).
- [18] Thwaites D. Accuracy required and achievable in radiotherapy dosimetry: Have modern technology and techniques changed our views? *J Phys: Conf Ser* 2013;444:2006. <https://doi.org/10.1088/1742-6596/444/1/012006>.
- [19] van der Merwe D, Van Dyk J, Healy B, Zubizarreta E, Izewska J, Mijnheer B, et al. Accuracy requirements and uncertainties in radiotherapy: a report of the International Atomic Energy Agency. *Acta Oncol* 2017;56:1–6. <https://doi.org/10.1080/0284186X.2016.1246801>.
- [20] LaCouture TA, Xue J, Subedi G, Xu Q, Lee JT, Kubicek G, et al. Small bowel dose tolerance for stereotactic body radiation therapy. *Semin Radiat Oncol* 2016;26:157–64. <https://doi.org/10.1016/j.semradonc.2015.11.009>.
- [21] Mescher H, Ulrich S, Bangert M. Coverage-based constraints for IMRT optimization. *Phys Med Biol* 2017;62:N460–73. <https://doi.org/10.1088/1361-6560/aa8132>.
- [22] Unkelbach J, Alber M, Bangert M, Bokrantz R, Chan TCY, Deasy JO, et al. Robust radiotherapy planning. *Phys Med Biol* 2018;63:22TR02. <https://doi.org/10.1088/1361-6560/aae659>.
- [23] Witte MG, van der Geer J, Schneider C, Lebesque JV, Alber M, van Herk M. IMRT optimization including random and systematic geometric errors based on the expectation of TCP and NTCP. *Med Phys* 2007;34:3544–55. <https://doi.org/10.1118/1.2760027>.
- [24] Greco C, Pares O, Pimentel N, Louro V, Moraes J, Nunes B, et al. Target motion mitigation promotes high-precision treatment planning and delivery of extreme hypofractionated prostate cancer radiotherapy: Results from a phase II study. *Radiother Oncol* 2020;146:21–8. <https://doi.org/10.1016/j.radonc.2020.01.029>.
- [25] Grimm J. Dose tolerance for stereotactic body radiation therapy. *Semin Radiat Oncol* 2016;26:87–8. <https://doi.org/10.1016/j.semradonc.2015.12.001>.
- [26] Hanna GG, Murray L, Patel R, Jain S, Aitken KL, Franks KN, et al. UK consensus on normal tissue dose constraints for stereotactic radiotherapy. *Clin Oncol (R Coll Radiol)* 2018;30:5–14. <https://doi.org/10.1016/j.clon.2017.09.007>.
- [27] Diez P, Hanna GG, Aitken KL, van As N, Carver A, Colaco RJ, et al. UK 2022 consensus on normal tissue dose-volume constraints for oligometastatic, primary lung and hepatocellular carcinoma stereotactic ablative radiotherapy. *Clin Oncol* 2022;34:288–300. <https://doi.org/10.1016/j.clon.2022.02.010>.
- [28] Timmerman R. A story of hypofractionation and the table on the wall. *Int J Radiat Oncol Biol Phys* 2022;112:4–21. <https://doi.org/10.1016/j.ijrobp.2021.09.027>.
- [29] Stroom J, Vieira S, Greco C. The effect of dosimetric and radio-sensitivity variation on dose constraints. S3508-11 *Radiother Oncol* 2024;194(Sup 1). <https://user-swnwdfm.cld.bz/ESTRO-2024-Abstract-Book/3515/>.
- [30] Stroom J, Gilhuijs K, Vieira S, Chen W, Salguero J, Moser E, et al. Combined recipe for clinical target volume and planning target volume margins. *Int J Radiat Oncol Biol Phys* 2014;88:708–14. <https://doi.org/10.1016/j.ijrobp.2013.08.028>.
- [31] van Elmpt W, Nijsten S, Petit S, Mijnheer B, Lambin P, Dekker A. 3D in vivo dosimetry using megavoltage cone-beam CT and EPID dosimetry. *Int J Radiat Oncol Biol Phys* 2009;73:1580–7. <https://doi.org/10.1016/j.ijrobp.2008.11.051>.